Supporting Information

ESIPT-modulated HBT-*o*-carborane Dyads with Efficient Aggregation-induced Emission and Acid-induced Discolouration Properties

Xueyan Wu†*, Chenxi Zhang†, Na Li, Yan Lv, Jinxia Chi, Jixi Guo*

State Key Laboratory of Chemistry and Utilization of Carbon Based Energy Resources; College of Chemistry, Xinjiang University, Urumqi, 830017, Xinjiang, PR China.

E-mail: Wuxy90@xju.edu.cn， jxguo1012@163.com

Table of Contents

1. Synthesis……..S2

2. UV-Vis absorption and fluorescence emission spectra……S3

3. DFT calculation……S8

4. NMR Spectra of all new compounds.……S13

5. References…….…….S18

1. Synthesis

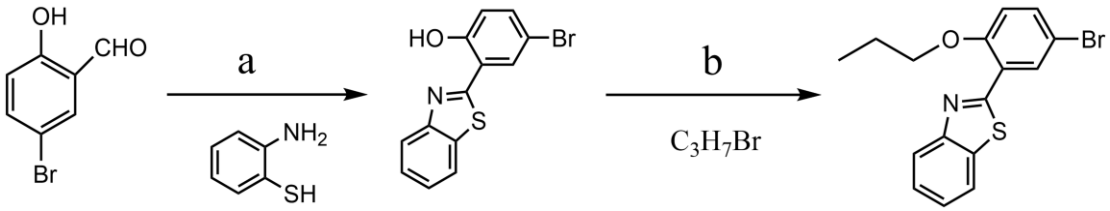

Scheme S1. synthetic routes for compounds **1** and **2**.

Compound 1: A solution of 2-aminothiophenol (4 mL, 4 mmol) and 5-bromosalicylaldehyde (800 mg, 4 mmol) in EtOH (10 mL), aqueous H_2O_2 (30%, 24.0 mmol) and aqueous HCl (37%, 15 mmol) was stirred for 6 h at ambient temperature. Then, the reaction was quenched with water (10 mL) and the organic layer was extracted with CH_2Cl_2 (3×30 mL) and dried over anhydrous $MgSO_4$. The solvent was removed under reduced pressure and the residue was purified by silica gel column chromatography using dichloromethane/petroleum ether (1/9, v/v) as the eluent to obtain target compound 1. The molecular structure characterisation results are in agreement with literature results.[1] Yield: 90%. ^{1}H NMR (400 MHz, $CDCl_3$) δ 12.53 (s, 1H), 8.01 (t, J = 14.4 Hz, 1H), 7.93 (t, J = 12 Hz, 1H), 7.80 (d, J = 7.2 Hz, 1H), 7.53 (t, J = 14.4 Hz, 1H), 7.48 – 7.42 (m, 2H), 7.01 (d, J = 10.4 Hz, 1H).

Compound 2: The mixture of compound 1 (4.896 g, 16 mmol), K_2CO_3 (3.980 g, 28.8 mmol) and N,N-dimethyl formamide (20 mL) were stirred at room temperature, then bromopropane (8.855 g, 72 mmol) was added. The mixture were stirred at 50 °C for 4 h. Then, the reaction was quenched with water (10 mL) and the organic layer was extracted with CH_2Cl_2 (3×30 mL) and dried over anhydrous $MgSO_4$. The solvent was removed under reduced pressure and the target compound 2 was obtained after drying. The molecular structure characterisation results are in agreement with

literature results.[2] Yield: 98%. ^{1}H NMR (400 MHz, $CDCl_3$) δ 8.71 (d, J = 6.4 Hz, 1H), 8.12 – 8.07 (m, 1H), 7.93 (t, J = 11.2 Hz, 1H), 7.53 – 7.47 (m, 2H), 7.39 (t, J = 14.4 Hz, 1H), 6.91 (d, J = 9.6 Hz, 1H), 4.15 (t, J = 14.4 Hz, 2H), 2.04 (t, J = 28 Hz, 2H), 1.18 (t, J = 18 Hz, 3H).

2. UV-vis absorption and fluorescence emission spectra

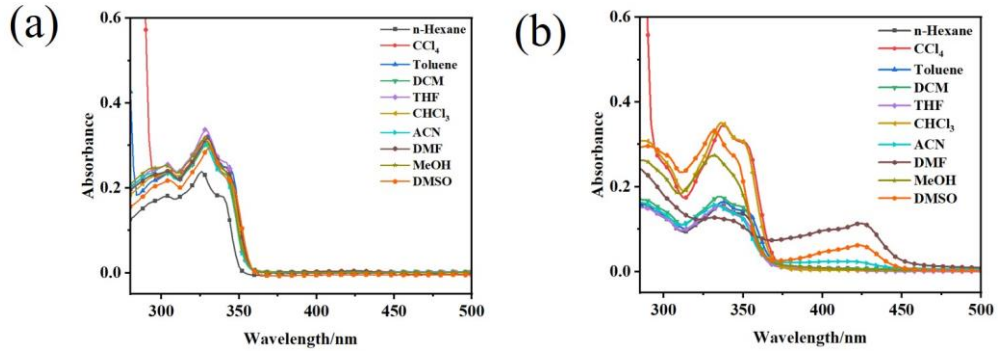

Fig. S1 UV-visible absorption spectra of compounds (a) **C-HBTP** (λ_{ex} = 327 nm), (b) **C-HBTO** (λ_{ex} = 335 nm) in different solvents (c = 1.0 × 10^{-5} M, 25 °C)

The simplest consideration for general solvent effect is the Lippert-Mataga equation, by assuming that same excited-state is involved in absorption and emission, and energy difference between the ground- and excited-state is only proportional to solvent orientation polarizability (Δf).

$$\Delta\nu = \frac{2\Delta f}{4\pi\varepsilon_0 hca^3}\left(\mu_e - \mu_g\right)^2 + constant \qquad (1)$$

$$\Delta f = \frac{\varepsilon - 1}{2\varepsilon + 1} - \frac{n^2 - 1}{2n^2 + 1} \qquad (2)$$

where $\Delta\nu = \nu_{abs} - \nu_{em}$ stands for Stokes' shift, ν_{abs} and ν_{em} are absorption and emission (cm^{-1}), h is the Planck's constant, c is the velocity of light in vacuum, a is the radius of the solvent cavity in which the fluorophore resides (Onsager cavity radius). Δf is the orientation polarizability, μ_e and μ_g is the ground-state dipole in the ground-state geometry and the excited dipole in the excited-state geometry and ε_0 is the permittivity of the vacuum.

Table S1. Absorption and emission spectra of **C-HBTP** and **C-HBTO**.[a]

Solvent	C-HBTP			C-HBTO			Δf
	λ_{abs}(nm)	λ_{em}(nm)	Stokes shift(cm^{-1})	λ_{abs}(nm)	λ_{em}(nm)	Stokes shift(cm^{-1})	
n-hexane	340	363, 510	1863, 9803	350	511	9002	0.001
Toluene	342	369, 511	2139, 9670	353	510	8843	0.014
DCM	343	370, 545	2127, 10805	352	508	8720	0.217
THF	342	369, 536	2139, 10583	351	528	8724	0.210
ACN	342	370, 576	2212, 11875	348, 420	-	9550	0.305
DMF	343	372, 572	2272, 11672	345, 424	-	-	0.275
MeOH	343	373, 548	2344, 10906	345	509	-	0.302
DMSO	344	377, 578	2544, 11768	346 424	-	9339	0.260

[a]Measured in various solution (1 × 10-3 M) at room temperature, C-HBTP (λ_{ex} = 327 nm), (b) C-HBTO (λ_{ex} = 335 nm), respectively.

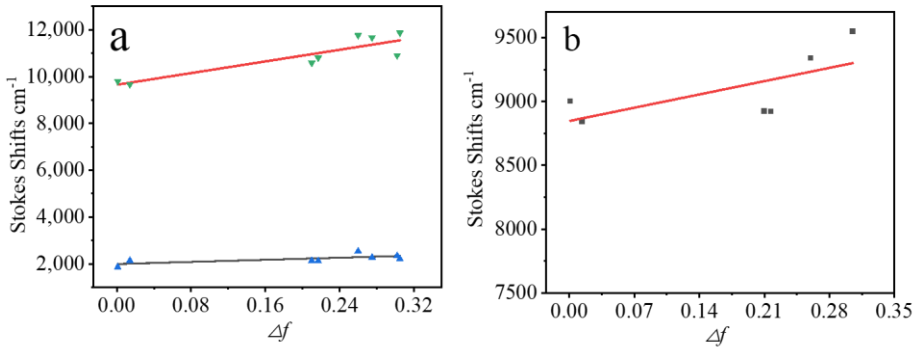

Fig S2. Lippert−Mataga plots of (a) **C-HBTP** and (b) **C-HBTO**.

It is known that the solvent polarity effect can be analyzed by the difference in the dipole moments of the ground and excited states, and the Stokes shift is proportional to the dipole moment change. This phenomenon can be elucidated using a Lippert–Mataga plot, which is a plot of the Stokes shift against the solvent polarizability, Δf [3,4,5]. As shown in Fig. S2, the slope of emission band around 350 and 530 nm are 1127 cm^{-1} 6226 cm^{-1} for **C-HBTP**, respectively. On the other hand, the slope of emission band around 530 nm for **C-HBTO** is 1486 cm^{-1}. These data indicate that the luminescent bands around 350 and 530 nm for **C-HBTP** should be assigned to the LE state and the ICT state, respectively. And further indicating that the weak electron interaction of *o*-carborane and HBT under the formed keto tautomer in **C-HBTO**. Besides, according to the Lippert−Mataga equation the dipole moment changes ($\Delta\mu$) for compounds **C-HBTP** and **C-HBO** were estimated to be 5.61 and 3.13 Debye, respectively. One Debye unit is 1.0 × 10^{-18} esu cm. 4.8 Debye is the dipole moment that results from a charge separation of one unit charge (4.8 × 10^{-10} esu) by 1 Å (10^{-8} cm) [6]. Therefore, the measured changes of the dipole moments forecast that one electron (unit charge) shifting a distance of ~1.17 Å for **C-HBTP**, which corresponding to the distance between the HBT donor and the

carbon atom of the *o*-carborane acceptor. But for **C-HBTO**, the dipole moment changes ($\Delta\mu$) is only 3.13 Debye less half than that of **C-HBTP**.

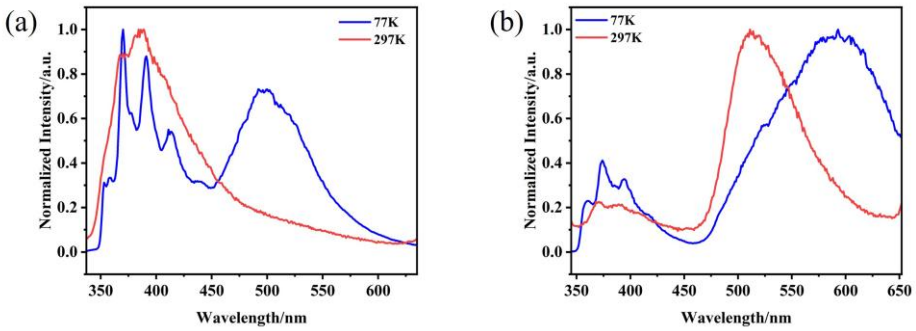

Fig. S3 The emission spectra of (a) **C-HBTP** (λ_{ex} = 327 nm) and (b) **C-HBTO** (λ_{ex} = 335 nm) in 2-MeTHF at r.t. and 77K, $c = 1.0 \times 10^{-5}$ M.

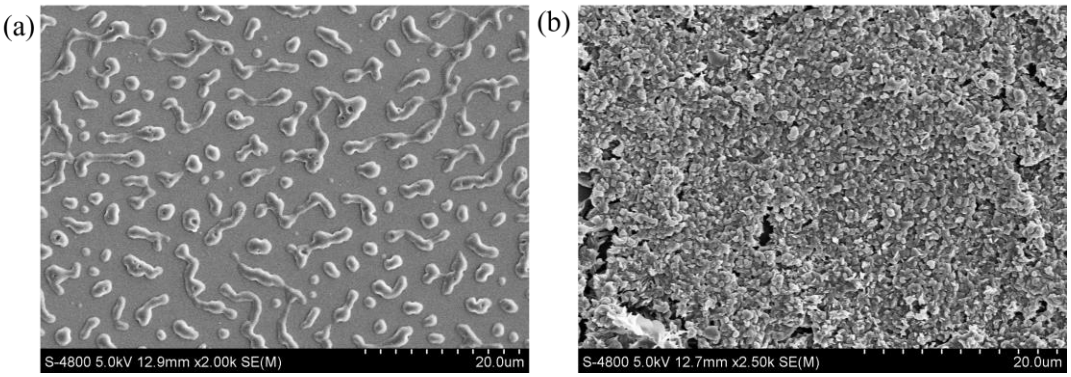

Fig. S4 SEM images of (a) C-HBTP and (b) C-HBTO at 99% f_w.

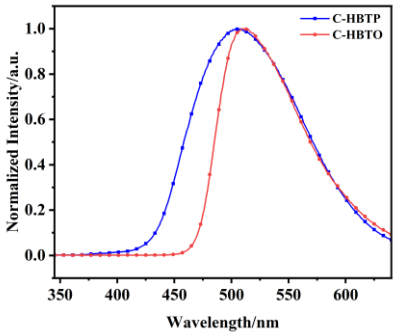

Fig. S5 Normalized solid-state luminescence spectra of **C-HBTP** (λ_{ex} = 327 nm) and **C-HBTO** (λ_{ex} = 335 nm) in the solid state.

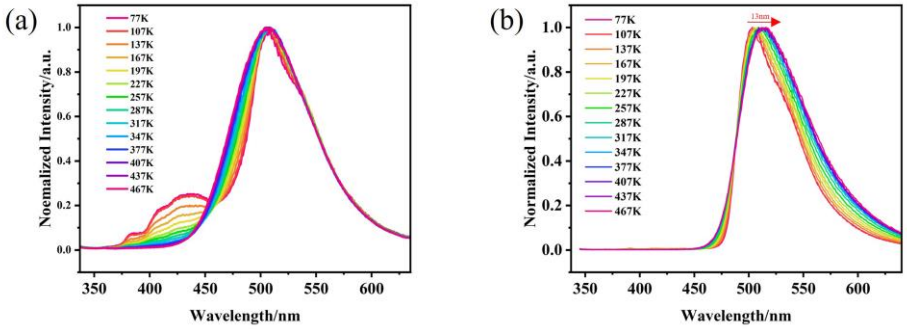

Fig. S6 Normalized temperature-dependent emission spectra of (a) **C-HBTP** (λ_{ex} = 327 nm) and (b) **C-HBTO** (λ_{ex} = 335 nm) in the solid state with temperature variation in the range of 77-467 K.

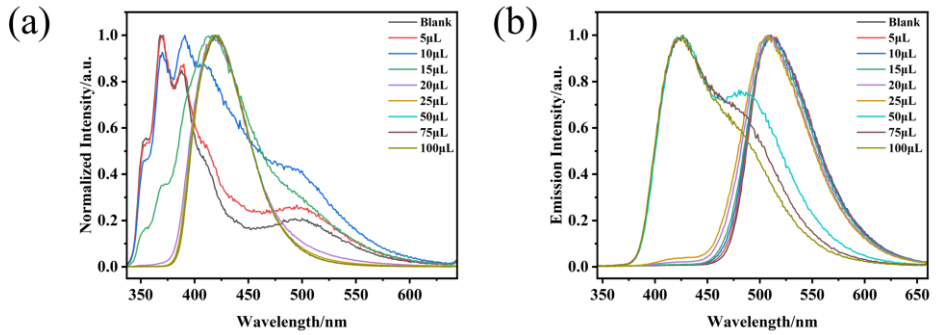

Fig. S7 Normalized luminescence spectra of (a) **C-HBTP** (λ_{ex} = 327 nm) and (b) **C-HBTO** (λ_{ex} = 335 nm) in CCl_4 at different trifluoroacetic acid concentrations.

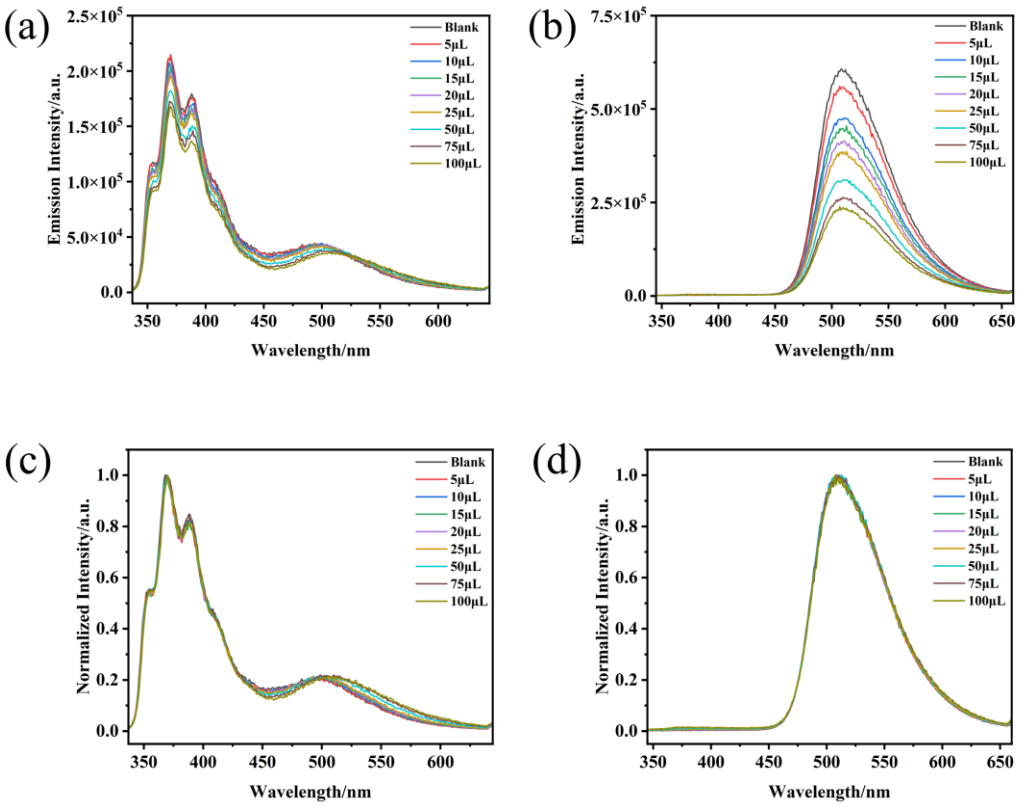

Fig. S8 Luminescence spectra of (a) **C-HBTP** (λ_{ex} = 327 nm) and (b) **C-HBTO** (λ_{ex} = 335 nm) in CCl_4 at different DMSO concentrations. Normalized luminescence spectra of (c) **C-HBTP** (λ_{ex} = 327 nm) and (d) **C-HBTO** (λ_{ex} = 335 nm) in CCl_4 at different DMSO concentrations.

3. DFT calculation

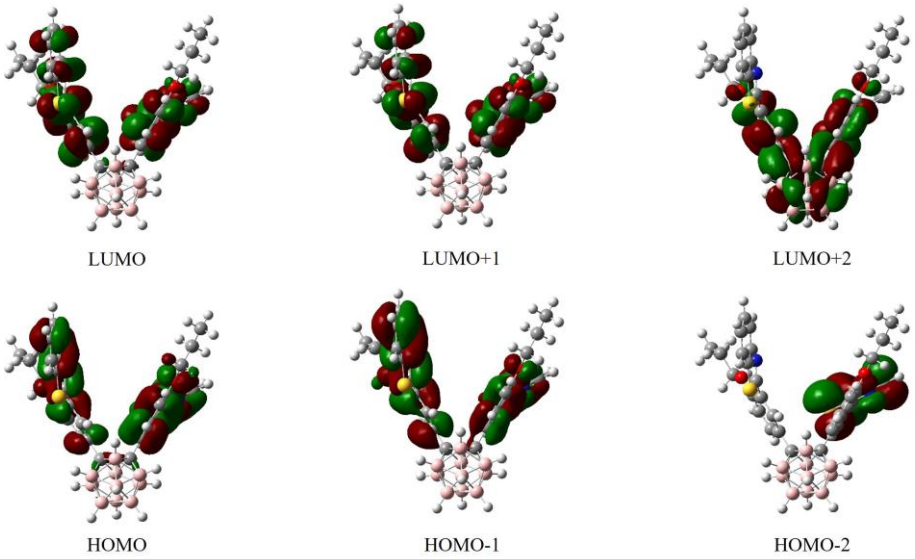

Fig. S9 The theoretical calculated ground-state frontier orbitals contributions of **C-HBTP** in gas sate using B3LYP/6-31G (d, p) level by Gaussian 09.

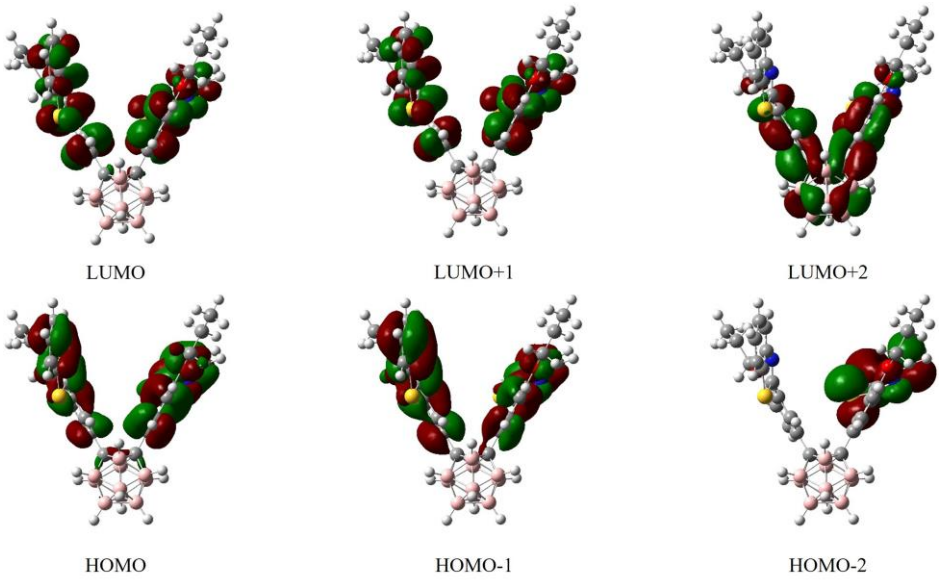

Fig. S10 The theoretical calculated UV-vis absorption frontier orbitals contributions of **C-HBTP** in gas sate estimated by TD-DFT calculation at the B3LYP/6-31G (d, p) level by Gaussian 09.

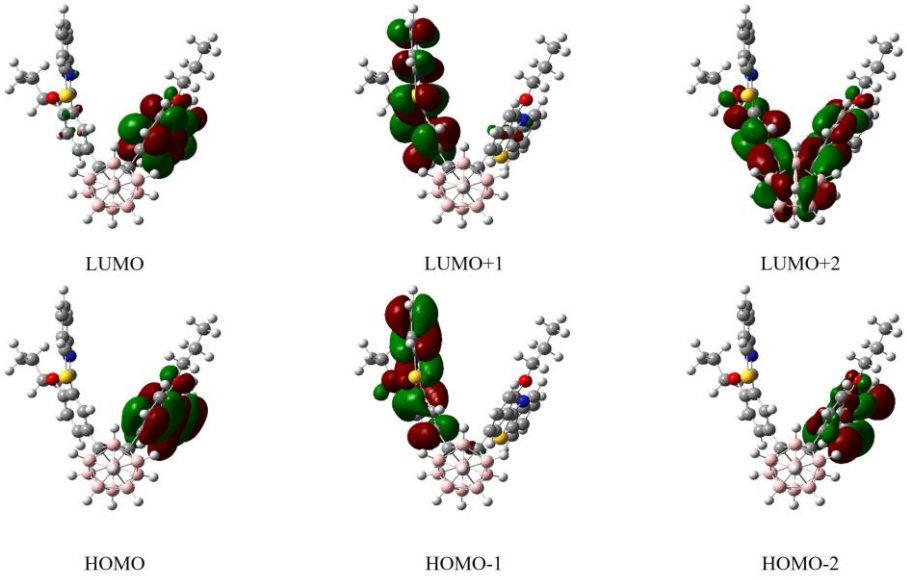

Fig. S11 The theoretical calculated singlet state (Fluorescence) frontier orbitals contributions of **C-HBTP** in gas sate estimated by TD-DFT calculation at the B3LYP/6-31G (d, p) level by Gaussian 09.

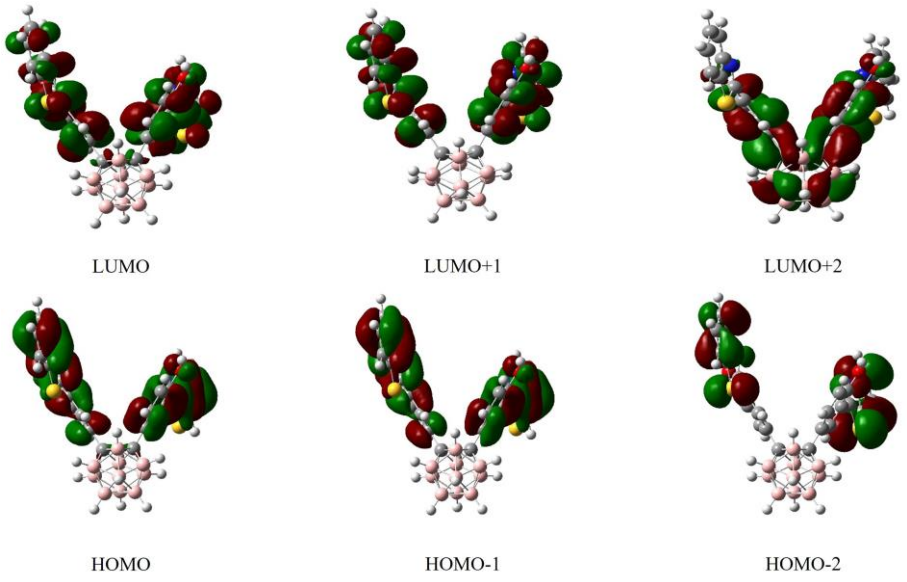

Fig. S12 The theoretical calculated ground-state frontier orbitals contributions of **C-HBTO** enol-type in gas sate using B3LYP/6-31G (d, p) level by Gaussian 09.

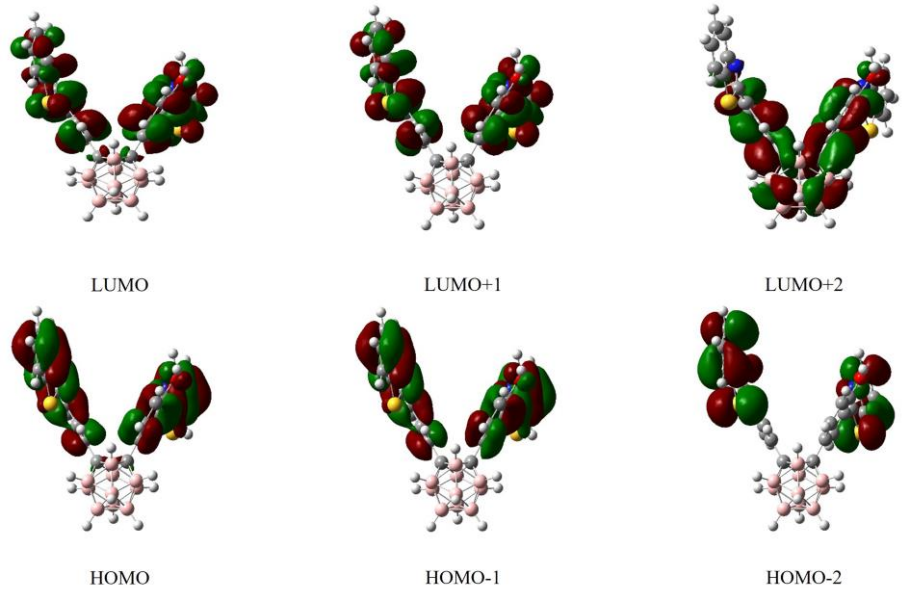

Fig. S13 The theoretical calculated UV-vis absorption frontier orbitals contributions of **C-HBTO** enol-type in gas sate estimated by TD-DFT calculation at the B3LYP/6-31G (d, p) level by Gaussian 09.

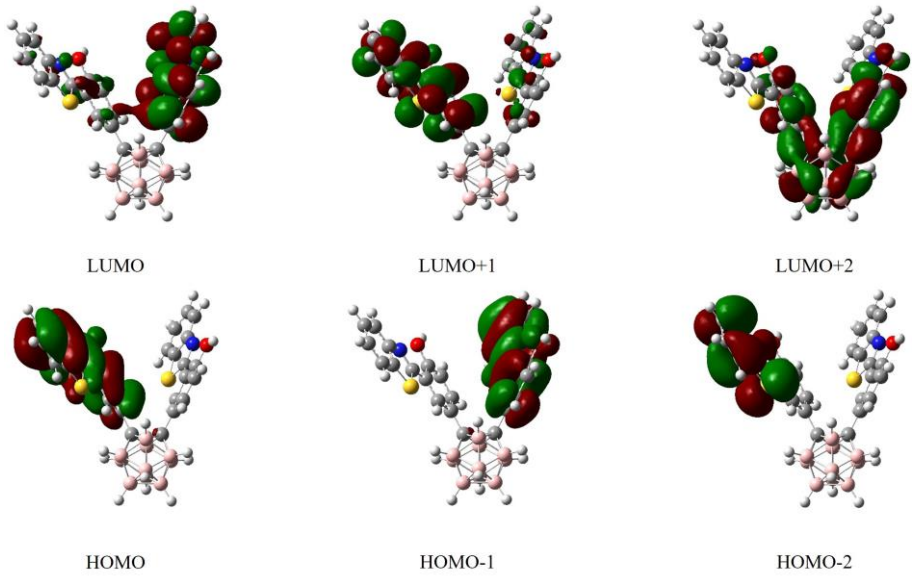

Fig. S14 The theoretical calculated singlet state (Fluorescence) frontier orbitals contributions of **C-HBTO** enol-type in gas sate estimated by TD-DFT calculation at the B3LYP/6-31G (d, p) level by Gaussian 09.

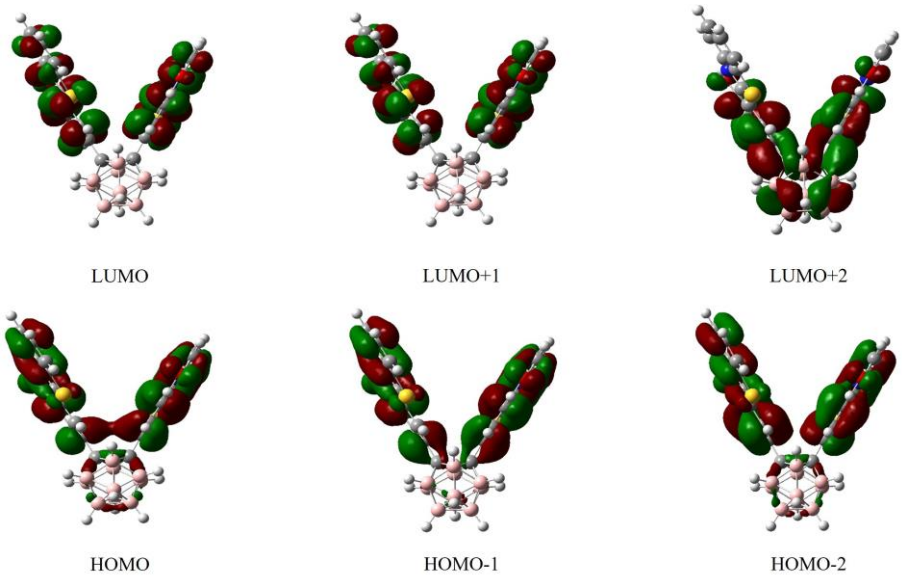

Fig. S15 The theoretical calculated ground-state frontier orbitals contributions of **C-HBTO** keto-type in gas sate using B3LYP/6-31G (d, p) level by Gaussian 09.

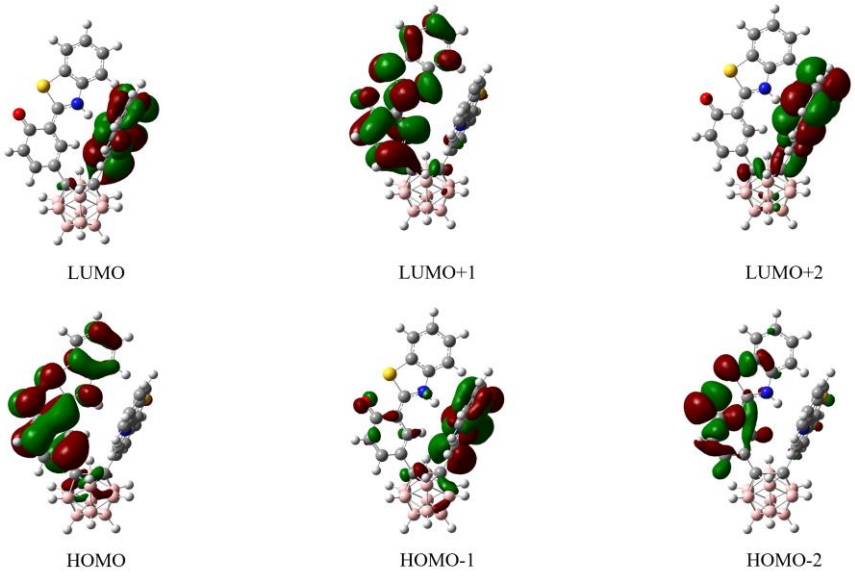

Fig. S16 The theoretical calculated UV-vis absorption frontier orbitals contributions of **C-HBTO** keto-type in gas sate estimated by TD-DFT calculation at the B3LYP/6-31G (d, p) level by Gaussian 09.

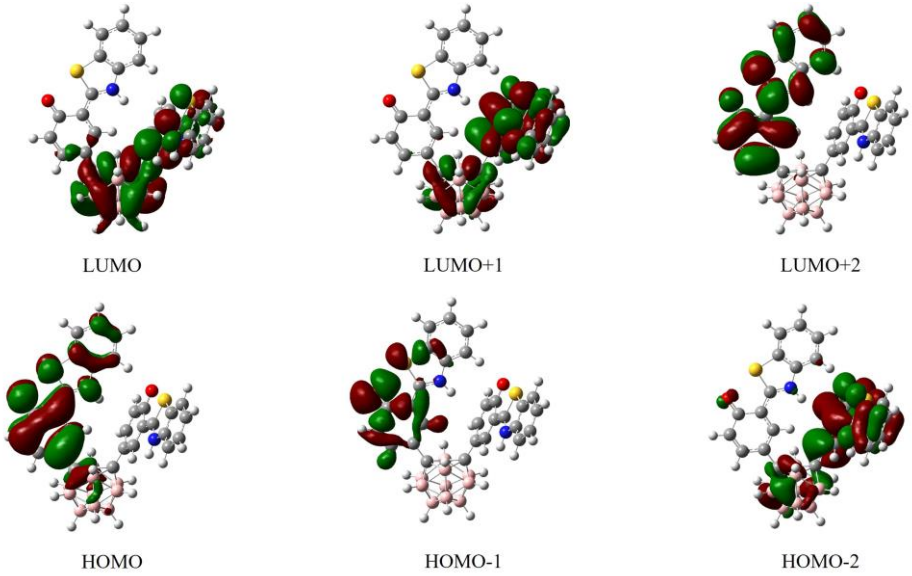

Fig. S17 The theoretical calculated singlet state (Fluorescence) frontier orbitals contributions of **C-HBTO** keto-type in gas sate estimated by TD-DFT calculation at the B3LYP/6-31G (d, p) level by Gaussian 09.

4. NMR Spectra of all new compounds

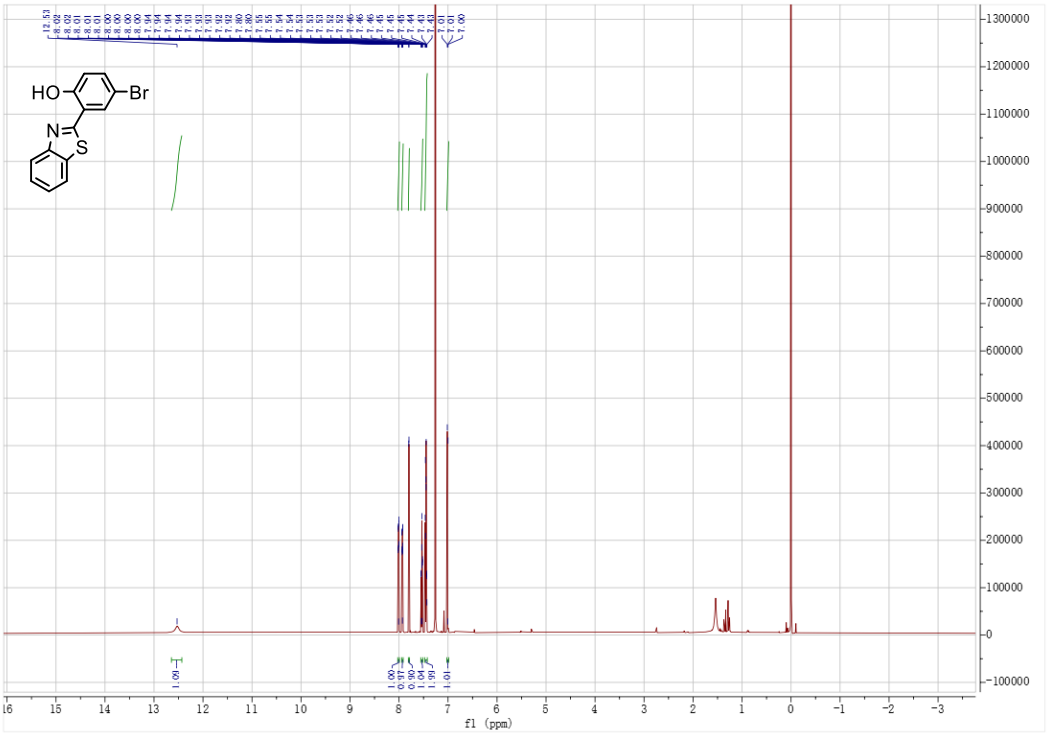

Fig. S18. ^{1}H NMR spectra of 2-(2-Benzothiazolyl)-4-bromophenol in $CDCl_3$.

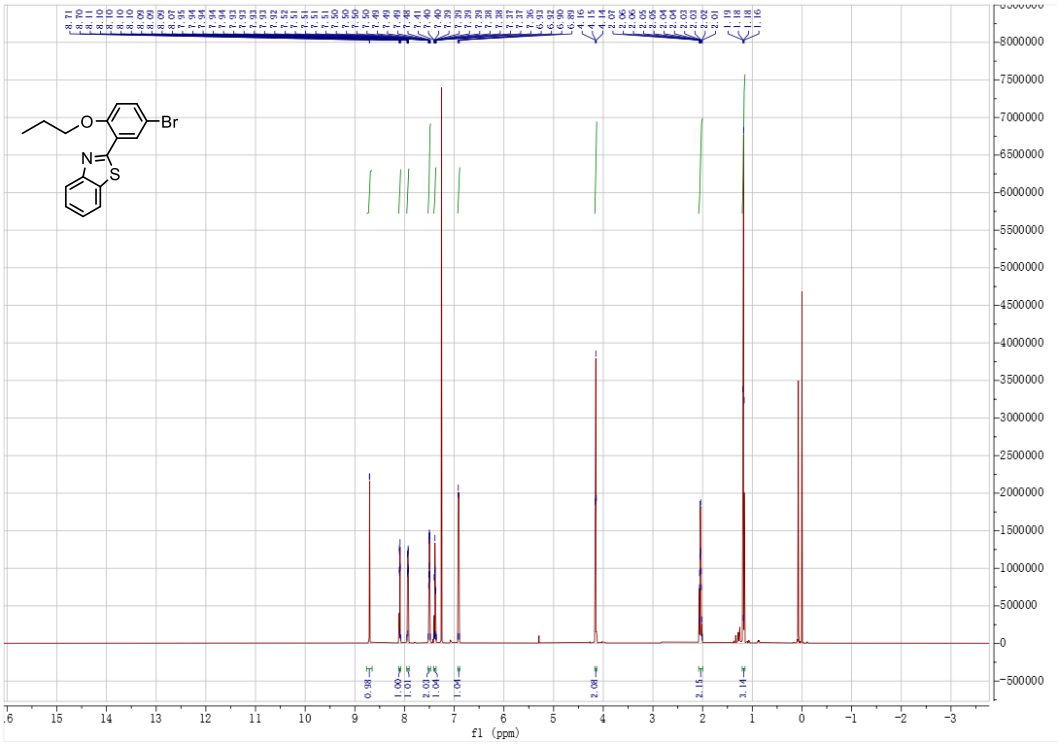

Fig. S19. ^{1}H NMR spectra of 2-(5-Bromo-2-propoxyphenyl)benzothiazole in $CDCl_3$.

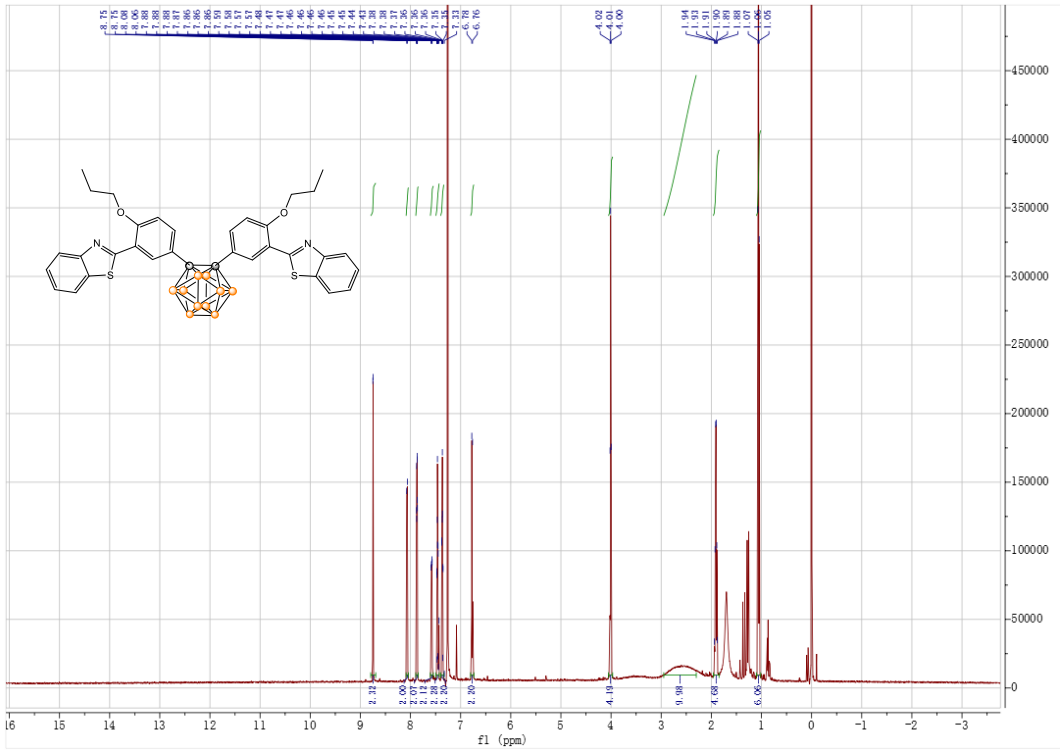

Fig. S20. ^{1}H NMR spectra of **C-HBTP** in $CDCl_3$.

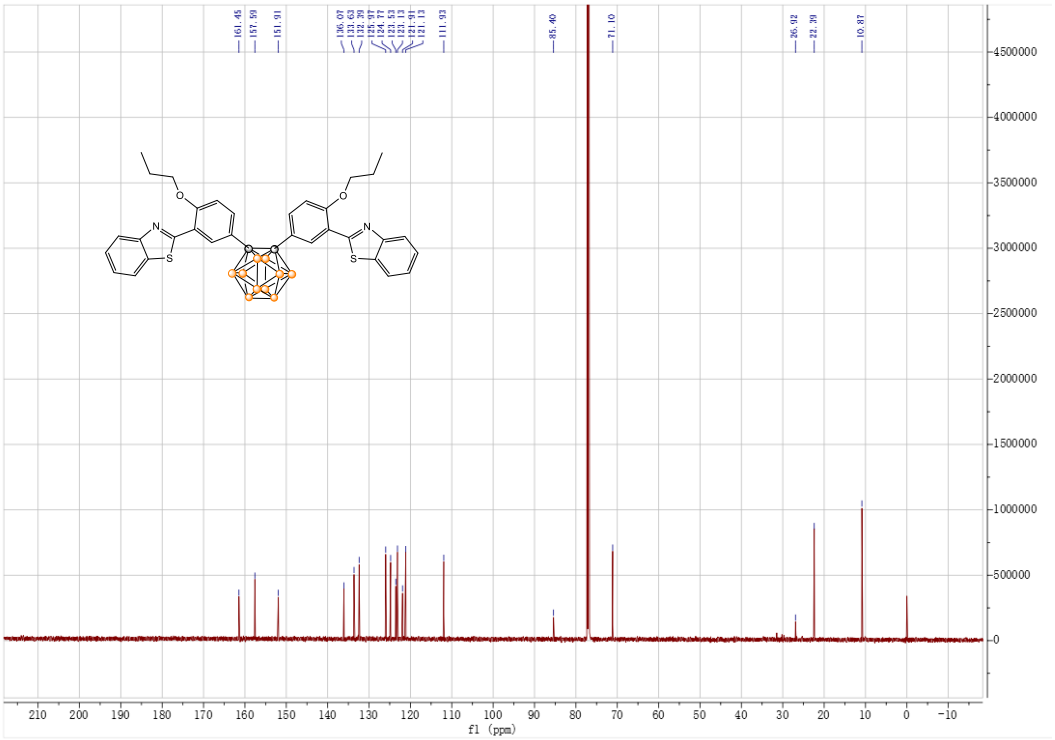

Fig. S21. ^{13}C NMR spectra of **C-HBTP** in $CDCl_3$.

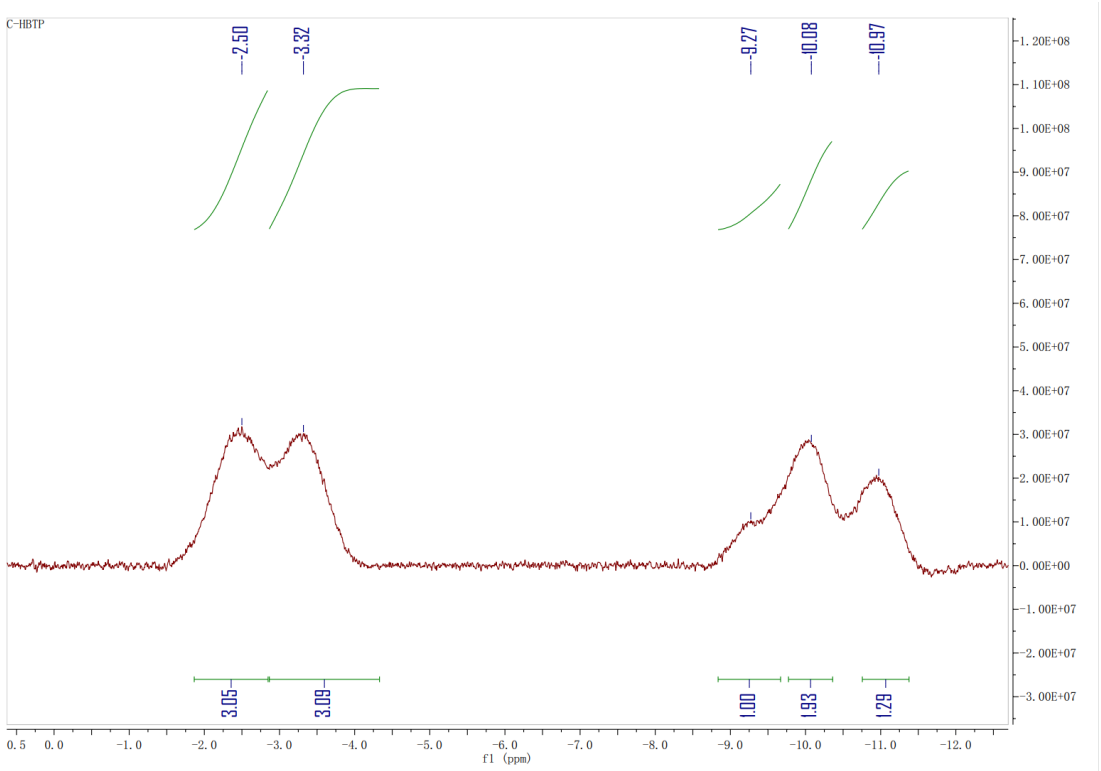

Fig. S22. ^{11}B NMR spectra of **C-HBTP** in Acetone-d6.

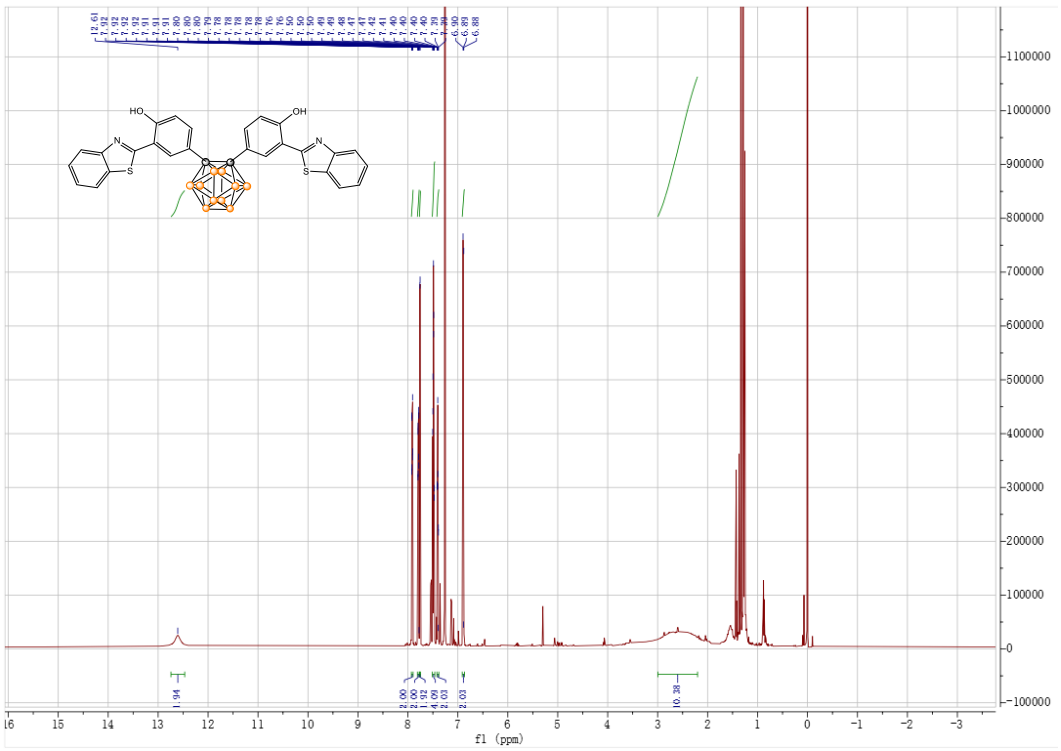

Fig. S23. ^{1}H NMR spectra of **C-HBTO** in $CDCl_3$.

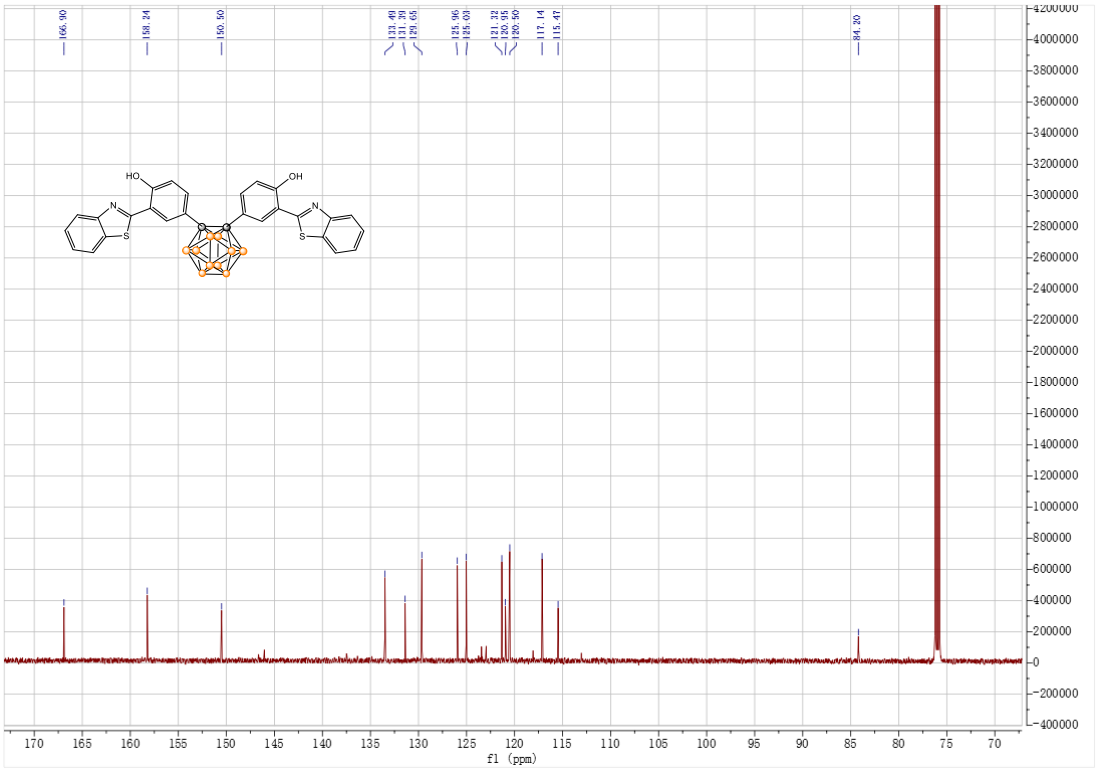

Fig. S24. ^{13}C NMR spectra of **C-HBTO** in $CDCl_3$.

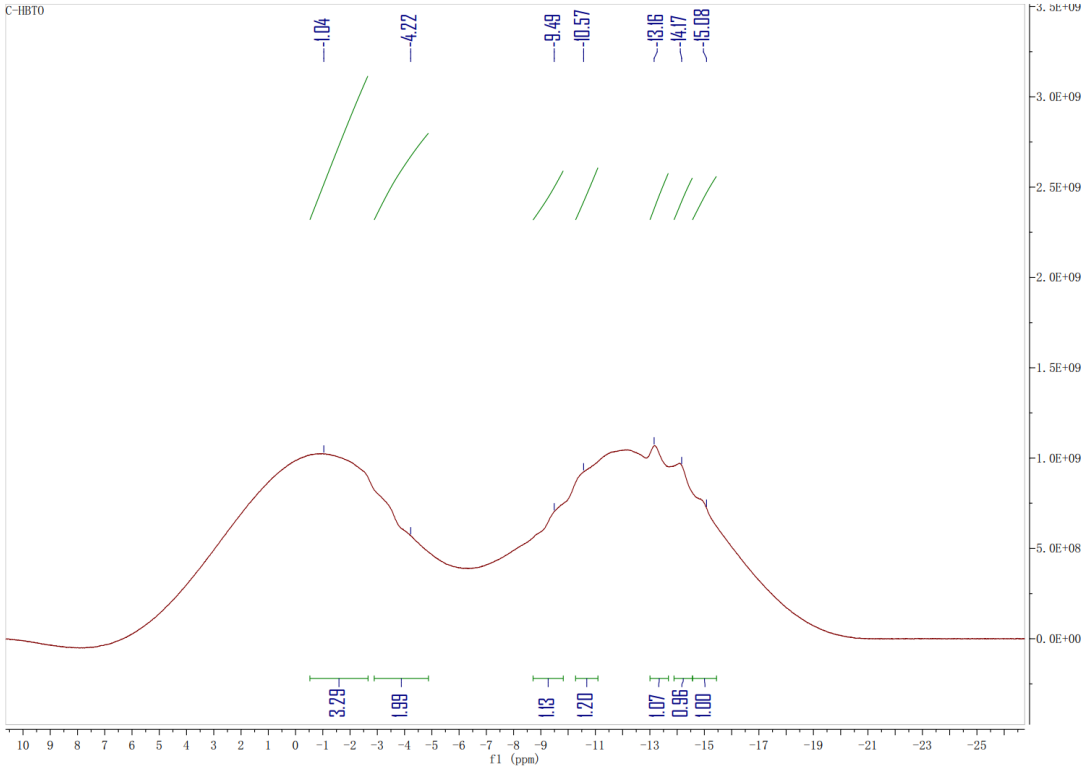

Fig. S25. ^{11}B NMR spectra of **C-HBTO** in Acetone-d6.

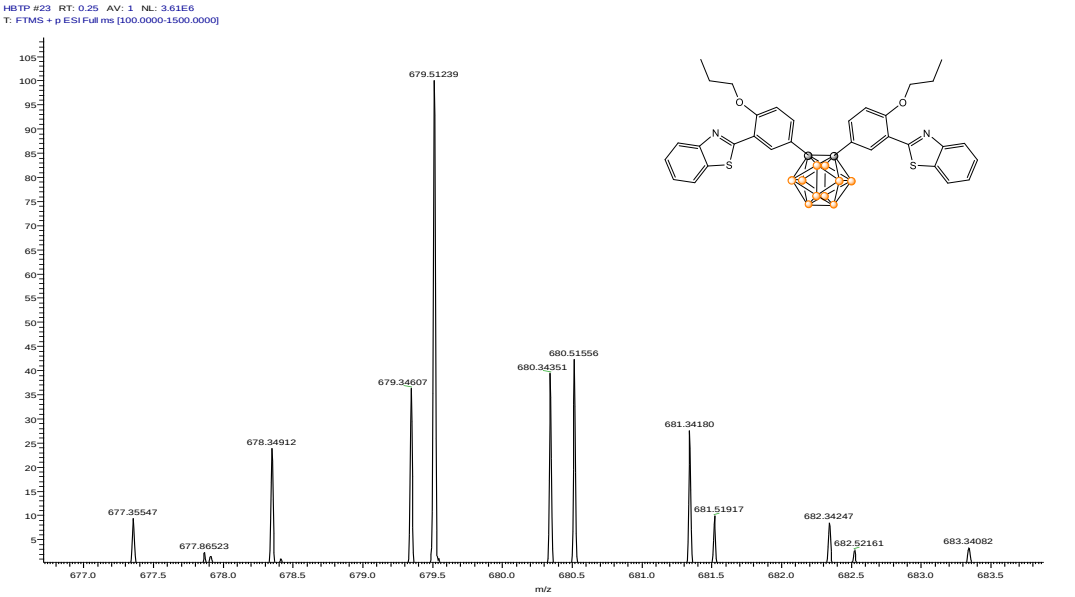

Fig. S26. The HRMS spectra of **C-HBTP**.

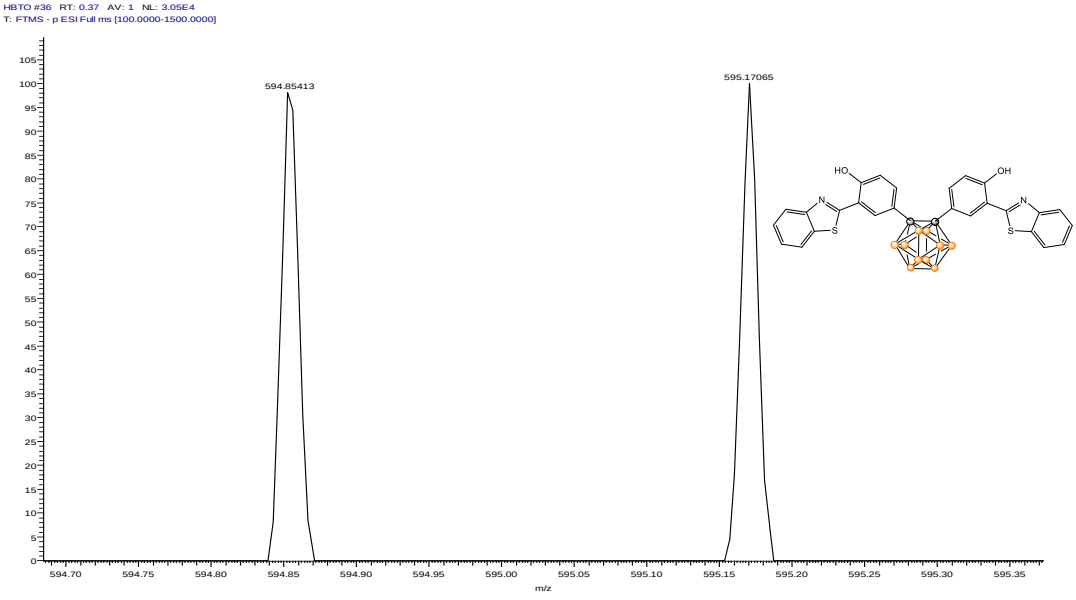

Fig. S27. The HRMS spectra of **C-HBTO**.

5. References

1 S. Paul, R. Nandi, K. Ghoshal, M. Bhattacharyya and D. K. Maiti, *New J. Chem.*, **2019**, 43: 3303-3308.

2 J. Ma, J. Zhao, P. Yang, D. Huang, C. Zhang and Q. Li, *Chem. Commun.*, **2012**, 48: 9720-9722.

3 J.R. Lakowicz Principles of fluorescence spectroscopy (3rd), Springer, Singapore (2010) ch.6

4 S.Y. Kim, Y.J. Cho, G.F. Jin, W.S. Han, H.J. Son, D.W. Cho, et al. Intriguing emission properties of triphenylamine–carborane systems Phys Chem Chem Phys, 17 (2015), pp. 15679-15682

5 Y.J. Cho, S.Y. Kim, M. Cho, W.S. Han, H.J. Son, D.W. Cho, et al. Kang. Aggregation-induced emission of diarylamino-π-carborane triads: effects of charge transfer and π-conjugation Phys Chem Chem Phys, 18 (2016), pp. 9702-9708

6 V. M. Divac et al. Spectrochimica Acta Part A: Molecular and Biomolecular Spectroscopy, 2019, 212, 356–362.